CrossMark

Phase relationship between summer and winter monsoons over the South China Sea: Indian Ocean and ENSO forcing

Yue Zhang[1] · Wen Zhou[1] · Marco Y. T. Leung[1]

Abstract

This paper identifies the seasonal relationships between monsoon activities over South China (SC) in winter and summer, which can help improve seasonal predictability. A predefined unified monsoon index that can well represent monsoon characteristics in both winter and summer over SC is employed. A time series of this unified monsoon index in summer and winter, and a lead-lag correlation analysis of the unified monsoon index, found that from summer to winter, monsoon activities tend to have an out-of-phase relationship (weak summer with strong winter monsoons or strong summer with weak winter), while from winter to summer, they tend to be in-phase (weak winter with weak summer or strong winter with strong summer). The composite difference between strong and weak winter monsoons shows that in the preceding summer of strong winter monsoons, monsoon activities tend to be weak, due to the influence of developing La Niña-like events; in the ensuing summer, monsoon activities tend to be strong, modulated by an anomalous cyclone over the western North Pacific (WNP), which is triggered by that La Niña-like pattern over the East Pacific. From summer to winter, the Indian Ocean dipole (IOD) mode is evident over the Indian Ocean (IO); from winter to summer, the Indian Ocean Basin (IOB) mode is dominant, which confirms the important role of the IO in these seasonal relationships of monsoon activities. A negative IOD pattern acts together with La Niña-like forcing, enhances northerly anomalies over East Asia, strengthens winter monsoon winds, and thus enhances the out-of-phase relationship. IOB cooling can capture the anomalous signal of El Niño–Southern Oscillation (ENSO) and favor the persistence of an anomalous cyclone over the WNP until the following summer ("capacitor effect"), which is important for the in-phase relationship. These roles are also further verified by numerical experiments that prescribe ENSO-like, IOD-like, and IOB-like heat source anomalies over the Pacific and IO in an anomalous atmospheric general circulation model.

Keywords Monsoon phase relationship · ENSO · Indian Ocean dipole · Indian Ocean basin mode

1 Introduction

In studies of climate variability and seasonal predictability in monsoon regions, it is of interest to identify the possible relationships between summer and winter monsoon activities. Establishing connections between seasons is important because it can potentially provide seasonal prediction of monsoon activities. Previous studies have suggested there are some seasonal linkages between summer and winter monsoons. Using the concept of "monsoon year," which

was first proposed by Yasunari (1991), and the season-reliant empirical orthogonal function (S-EOF) method, Wang et al. (2008) found that the leading mode of Asian–Australian monsoon (AAM) variability exhibits a prominent biennial tendency that can cover a whole monsoon year, from one summer to the following summer. In terms of the phase relation between monsoon seasons, previous studies have made preliminary conclusions regarding intensity connections in the East Asian monsoon region from summer to winter, where there tends to be an out-of-phase relation. However, from winter to summer, the seasonal relationship tends to be more variable (Chen et al. 2000; Chang et al. 2000; Wu and Chan 2005a; Li et al. 2010; Feng and Chen 2014; Wu et al. 2014). For example, Wu and Chan (2005a) classified summer and winter monsoon years into different categories according to monsoon intensity and found

✉ Wen Zhou
wenzhou@cityu.edu.hk

[1] Guy Carpenter Asia-Pacific Climate Impact Center, School of Energy and Environment, City University of Hong Kong, Tat Chee Ave., Kowloon, Hong Kong, SAR, China

that a stronger summer monsoon preceded a weaker winter monsoon (out-of-phase relationship) and a weaker winter monsoon was followed by a stronger summer monsoon (out-of-phase relationship), and this was under the influence of the transition of ENSO from a positive to a negative phase. But Li et al. (2010) used a newly defined monsoon index to identify an in-phase relationship between strong (weak) East Asian winter monsoons and ensuing strong (weak) summer monsoons. Using EOF analysis, Wu et al. (2014) also found cross-seasonal connections in rainfall variability over the South China Sea (SCS) region; leading summer and winter were out-of-phase, while winter and ensuing summer were in-phase, but the focus was only on the ocean.

However, the mechanism behind this connection is so complex that it is hard to draw a simple conclusion. Previous works have clarified the role of the ENSO in this relation (Chen et al. 2000; Wu and Chan 2005a; Chan and Zhou 2005; Zhou and Chan 2007; Wang et al. 2008; Zhou et al. 2009b; Feng and Chen 2014; Wu et al. 2014; Leung et al. 2017). During the summer of El Niño development, remote ENSO forcing plays a major role in the monsoon system anomalies that exhibit a tilted anticyclonic ridge that originates in the Maritime Continent and strengthens the western North Pacific (WNP) monsoon (Wang et al. 2003). And a warm ENSO event can weaken the East Asian winter monsoon through remote response and teleconnection (Li 1989; Chang 2004). From winter to summer, El Niño events can trigger a statistically significant occurrence of an anomalous anticyclone over the Philippine Sea during the mature winter. This anomalous anticyclone can persist from winter to the ensuing summer (Wang et al. 2000), and it is an important atmospheric system that conveys El Niño impact to the East Asian summer climate (Li et al. 2017). Chen et al. (2013) have also investigated the variations of these seasonal relationships under different combinations of ENSO and the Pacific decadal oscillation (PDO). Zhou et al. (2009b) demonstrated the SST forcing mechanisms for the leading biennial mode of AAM and suggested that besides ENSO forcing, local air–sea coupling effects can also play important roles in the seasonal evolution of monsoon activities. Li et al. (2010) hypothesized a possible tropospheric biennial oscillation mechanism to explain these seasonal relationships of monsoon activities. However, besides the factors already identified, other factors may also be vital in this seasonal relation. For example, studies on the modulation of Indian Ocean (IO) forcing on the seasonal relations of monsoon activities are limited. But the impact of IO on monsoon circulation cannot be neglected. For example, Wu et al. (2009) found that IO basin warming during the ENSO decaying summer is very important in maintaining the anticyclonic circulation over the WNP so that the anomalous atmospheric signals can pass through winter to summer. Xie et al. (2009) have addressed this effect of IO warming on the

following summer monsoon circulation as the IO capacitor effect, which can act together with local sea surface cooling in the easterly trade regime of the WNP to influence climate variability (Xie et al. 2016; Wang et al. 2013). This impact of IO basin warming has also been demonstrated by previous numerical model experiments (e.g., Lau and Nath 2003; Lau et al. 2006; Li et al. 2008; Zhou et al. 2009a). From a seasonal perspective, Wang and Wu (2012) discussed the IO forcing effect on the seasonal linkage, assuming a dominant in-phase relationship from winter to summer. But they did not discuss whether the IO played a role in modulating the relationship between the preceding summer and the following winter monsoons and what the relative roles of ENSO and IO are. Since the strong dependence between the ENSO and IO forcing modes cannot be ignored (Yuan et al. 2008c; Yang et al. 2015), and the detailed coupling effects between ENSO and the Indian Ocean dipole (IOD) or Indian Ocean Basin (IOB) modes are still not clear, it is important to investigate their relative roles in modulating the monsoon systems. So the ways in which IO forcing modulates these seasonal connections need further study.

In this study, a systematic framework is proposed to summarize the seasonal relationships of monsoon intensities between different seasons over South China (SC) and also to investigate the different roles ENSO and IO play in seasonal connections, and then to discuss the mechanism of these seasonal connections. The rest of this paper is organized as follows. In Sect. 2, the data and monsoon index used in this study are described. In Sect. 3, the phase relation between the summer and winter monsoons is examined and summarized. In Sect. 4, the forcing effects of ENSO, IOD, and IOB are investigated. In Sect. 5, numerical simulation is conducted to test the ENSO, IOD, and IOB forcing effects. In Sect. 6, a summary and discussion are given.

2 Data and meteorology

Gauge-based station precipitation and temperature data over stations in China are used in this study. For reanalysis data, the ERA-Interim dataset is employed here, which is produced by the European Centre for Medium-Range Weather Forecasts (ECMWF) (Dee et al. 2011). The gridded ($0.75° \times 0.75°$) monthly horizontal winds, geopotential height, omega, temperature, and sea surface pressure from 1979 to 2014 are used. The monthly mean National Oceanic and Atmospheric Administration (NOAA) optimum interpolation version 2 sea surface temperature (SST) with a resolution of $1° \times 1°$ (Reynolds et al. 2002) is also used. Outgoing longwave radiation (OLR) with a resolution of $2.5° \times 2.5°$ is used to represent tropical convection, which is based on the High Resolution Infrared Radiation Sounder (HIRS) v2r2 (Lee et al. 2007). Daily and monthly datasets

from the National Centers for Environmental Prediction/National Center for Atmospheric Research (NCEP/NCAR) are also used to calculate apparent heating, with a horizontal resolution of $2.5° \times 2.5°$ (Kalnay et al. 1996).

In order to represent the East Pacific (EP) and IO forcing modes, we employ the Niño-3.4 index to measure ENSO [the regional monthly-mean sea surface temperature over the region (5°S–5°N and 120°W–170°W)]; the DMI index to measure the IOD [the SST anomaly difference between the IODW region (10°S–10°N, 50°E–70°E) and the IODE region (10°S–0°S, 90°E–110°E)]; and the IOB index to measure the IOB [time series of the first mode of EOF analysis of SST anomalies (SSTAs) over the IO]. All these indices are calculated using the seasonal mean to deduct the sub-seasonal signals.

This study uses the unified monsoon index for SC to represent the intensity of monsoon activities. This unified index is proposed to analyze the climate variability of SC monsoons based on the idea that although wind direction reverses in different seasons, both the summer and winter monsoons are driven by the same mechanism, the north–south temperature contrast. In both winter and summer, the meridional winds at low levels over the SCS are the strongest in the entire East Asian monsoon system. Using meridional wind of the SCS as a unified index can well represent the monsoon features of both monsoon seasons. Therefore, 1000 hPa meridional wind averaged over the northern SCS (7.5°N–20°N, 107.5°E–120°E, shown as the box in Fig. 1) is adopted as the unified monsoon index for SC, which has been verified to be well related to summer rainfall as well
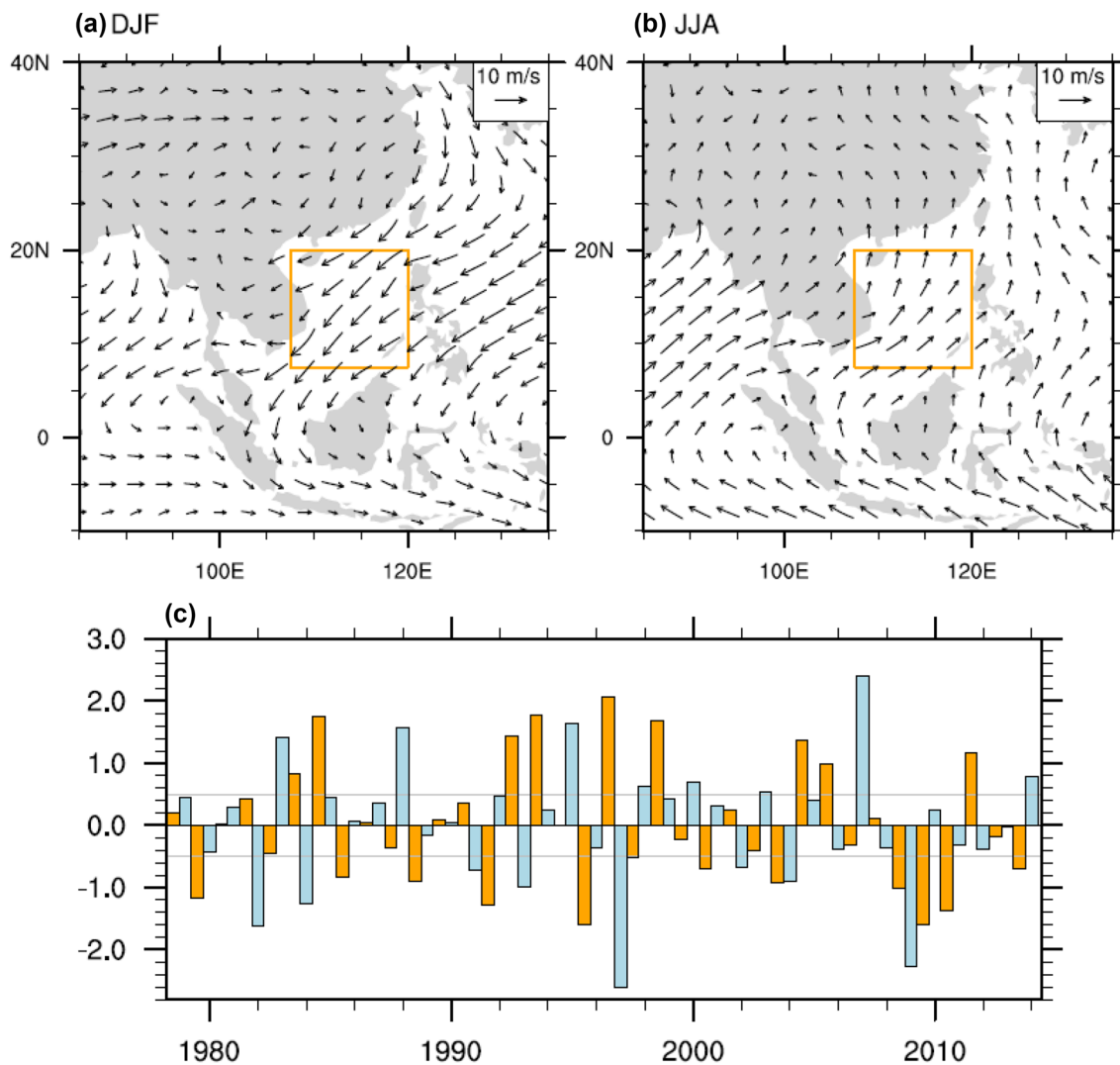

Fig. 1 Climatological 1000 hPa wind field during **a** winter and **b** summer; **c** time series of unified monsoon index (regional average of 1000 hPa meridional winds over 7.5°N–20°N, 107.5°E–120°E, shown by the yellow rectangular box in **a** and **b**). The light blue and orange bars (**c**) indicate the unified monsoon index during winter and summer, respectively

as winter temperature over SC based on station datasets (Lu and Chan 1999). As Lu and Chan (1999) defined, the averaged meridional wind fields of JJA are used to represent the summer monsoon, while those of NDJF are used to reflect the winter monsoon, which are the months when maximum summer southerly flow and maximum winter northerly flow are all located over the SCS. In this study, we follow the definition of this unified monsoon index, but when analyzing the winter circulation pattern, the DJF season is mainly used according to the convention of Asian monsoon research. The seasonal pattern of winds is shown in Fig. 1, where northerlies prevail over East Asia (EA), with an anomalous cyclonic circulation pattern over the Philippine Sea during winter, while southerlies prevail over the SCS during summer.

In order to test the performance of this index in representing the SCS monsoon system, correlation analysis is used here, and results are shown in Fig. 2. The correlation map of precipitation (Fig. 2a, c) shows that a positive precipitation center is located over the equatorial region and its negative center dominates EA during winter, which means that strong winter monsoons over the SCS correspond to less rainfall north of 20°N but more rainfall over the Maritime Continent (Fig. 1a). For temperature during winter, we can also see that negative correlations are dominant over this region, signifying the cold traits of winter monsoon activity. During summer, the correlation map of precipitation shows that SC and the northern SCS experience more precipitation, while the Yangtze River valley experiences less precipitation. The temperature pattern during summer is almost the opposite of the precipitation pattern. So, correlation analysis indicates that a strong winter monsoon features cold temperatures and less precipitation over SC and the northern SCS; and a strong summer monsoon features more precipitation over SC and the SCS, but less precipitation along the
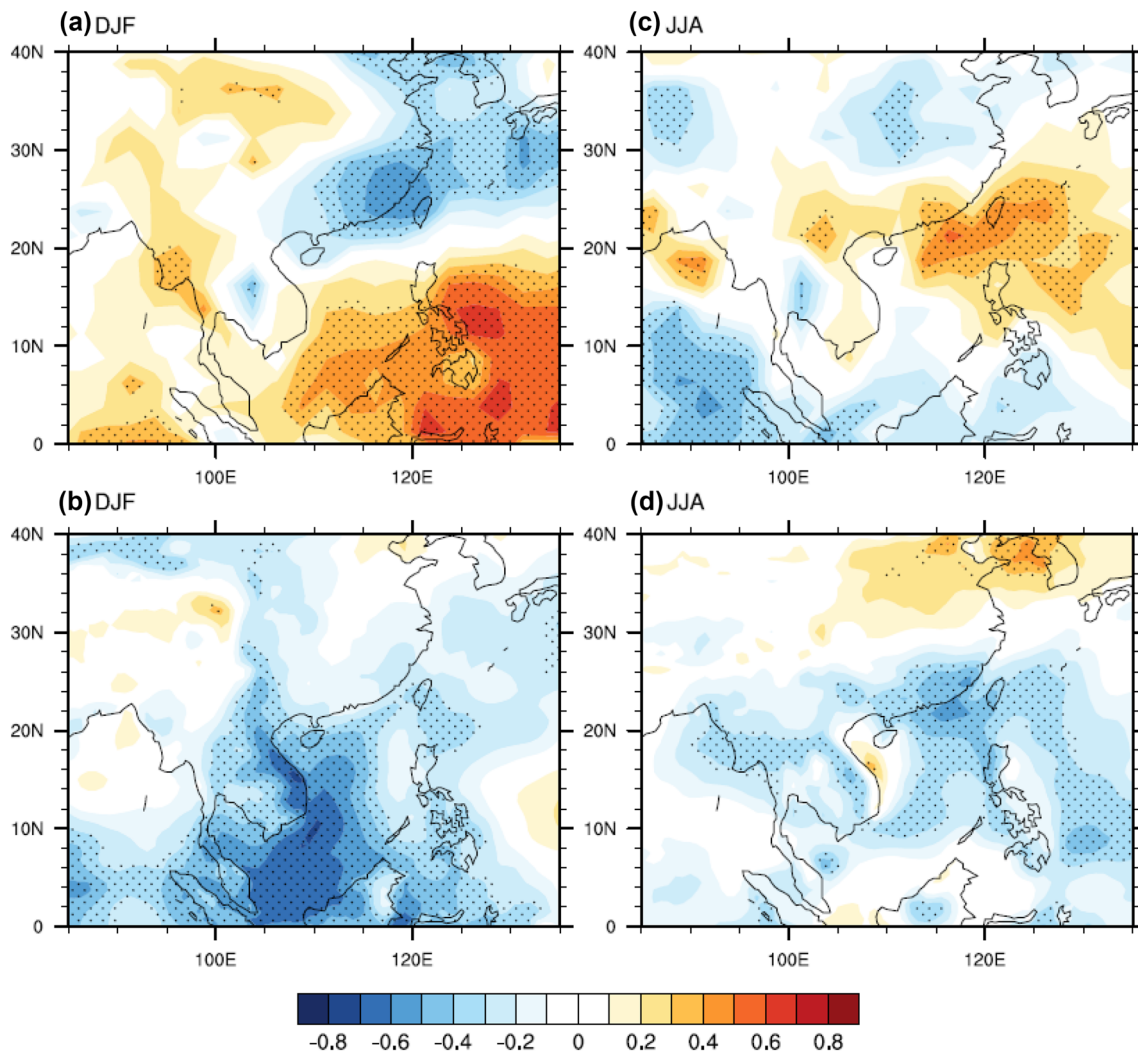

Fig. 2 Correlation maps of winter and summer **a, c** precipitation and **b, d** temperature regarding the unified monsoon index for 1979–2014. Dotted areas are statistically significant at the 95% confidence level

Meiyu-Baiu band, which is also consistent with the findings of other studies using different monsoon indices (Wang and Wu 2012).

This study uses the unified monsoon index during summer and winter to do lead-lag correlation analysis to identify the seasonal connection of monsoon activities between different seasons. In addition, composite analysis is also used to reveal monsoon circulation differences during the preceding and ensuing summer associated with strong and weak winter monsoon years to document the seasonal relationship from summer and winter and that from winter to summer. In order to test these seasonal linkages, an anomaly atmospheric general circulation model (AGCM) (Li 2006) based on the Princeton dynamic core is employed.

3 Phase relationships between summer and winter

Previous studies have suggested seasonal connections in rainfall variability over the SCS between summer and winter (Wu and Chan 2005b; Li et al. 2010; Wu et al. 2014), but without a consensus on whether a strong (weak) winter leads to a weak (strong) subsequent summer, or whether a strong (weak) winter leads to a strong (weak) subsequent summer. Figure 1c shows the time series of the unified monsoon index during winter (NDJF) and summer (JJA) for the period of 1979–2014. Because northerly winds are dominant during winter, the unified index is shown as negative. In order to compare the intensities of monsoons directly, the absolute value of the unified monsoon index is adopted for winter in Fig. 1c. According to the time series of the unified monsoon index for winter and summer in Fig. 1c, 21 of 36 years can be identified as out-of-phase (weak to strong or strong to weak) from summer to winter, indicating that the out-of-phase relation is dominant. But for cases in which winter leads summer, 19 of 36 years are in-phase (weak to weak or strong to strong), which might be consistent with previous studies (Li et al. 2010; Wu et al. 2014), but different from the work of Wu and Chan (2005a).

3.1 South China winter monsoon index

Using the unified monsoon index during winter correlated with lead-lag seasonal 850 hPa winds and the outgoing longwave radiation (OLR) fields (Fig. 3) from the preceding summer (JJA(−1)) to the following summer (JJA(0)), monsoon circulation relationships between different seasons can be further verified. The numbers −1 and 0 in parentheses signify whether the season belongs to the preceding or the same year as the January and February of that winter. During JJA(−1) (Fig. 3a), an anomalous anticyclonic circulation pattern is located over the western North Pacific, leading
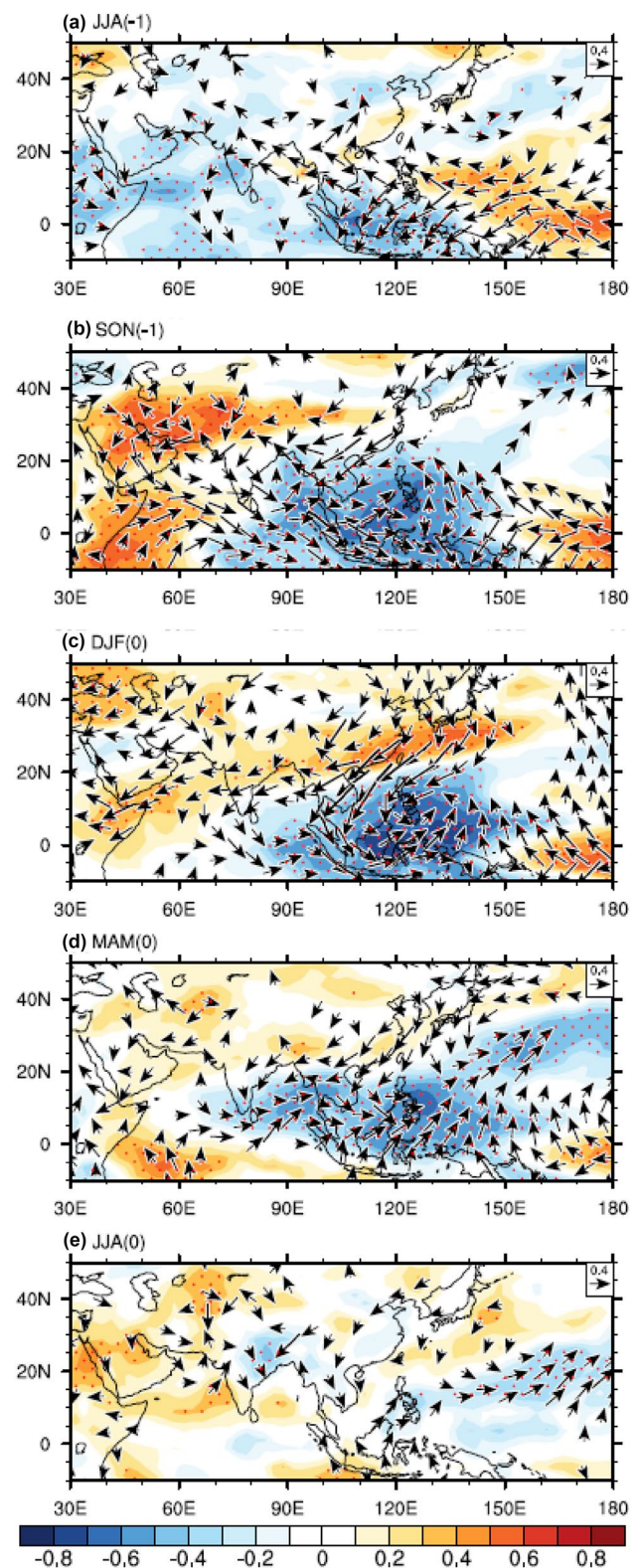

Fig. 3 Distribution of correlation coefficients of 850 hPa winds and OLR in lead-lag seasons with respect to the unified monsoon index for winter. Dotted areas are statistically significant in OLR fields at the 95% confidence level. Vectors indicate that the correlation coefficients of winds exceed the 95% confidence level

to southerly winds prevailing to its northwest. Associated with lower-tropospheric signals, a positive convection signal controls North China but a negative convection signal dominates SC and the SCS, which suggests that monsoon activity is suppressed over SC and the SCS during the preceding summer. During autumn (Fig. 3b), the convection center extends and northerly winds emerge over SC. In the simultaneous winter correlation maps (Fig. 3c), we can see that an anomalous cyclone controls the Philippines and the Maritime Continent, and to the north of this cyclone, northerly anomalous winds prevail, thus enhancing the climatological monsoon winds. Negative OLR values can be seen over the same region as that anomalous cyclone; however, the positive maximum shown as a belt dominates SC. Together, the wind fields and the OLR signals illustrate what a strong winter monsoon pattern looks like.

During MAM (0) (Fig. 3d), the positive OLR center disappears but the negative values are still evident and move northward, associated with cyclonic circulation signals, which also shift northward to the western North Pacific (WNP). During the ensuing summer, the cyclone pattern persists over the WNP, and to its west, negative OLR values affect SC, so the lower troposphere is favorable for monsoon convection, which is also indicated by weak negative OLR values over eastern China.

These seasonal evolution patterns are also compared with the work of Wang et al. (2008) and Zhou et al. (2009b), who used season-reliant EOF (S-EOF) analysis to identify the leading modes of Asian–Australian monsoon rainfall variations. Basically, Fig. 3 shows the opposite patterns with the first biennial mode of S-EOF results from their work, which also revealed a tendency of seasonal linkages between different monsoon seasons.

Based on the time series of the unified monsoon index during winter and the correlations of the monsoon system regarding the winter monsoon index, the seasonal relationships over SC can be summarized: that is, from summer to winter, monsoon activities tend to have an out-of-phase relation, and from winter to summer, they tend to have an in-phase relation.

3.2 South China summer monsoon index

Similarly, the unified monsoon index for summer (JJA) can also reproduce seasonal relationships between summer and winter. Correlation maps of the summer monsoon index with a lead-lag seasonal circulation pattern but from the current summer (JJA(0)) to the next summer(JJA(+1)) are shown in Fig. 4. The number + 1 in parentheses signifies that the season belongs to the ensuing year of that summer. Basically, Fig. 4 shows opposite patterns compared to Fig. 3, but it represents similar seasonal relations. During JJA(0) (Fig. 4a), a positive convection signal, indicated by
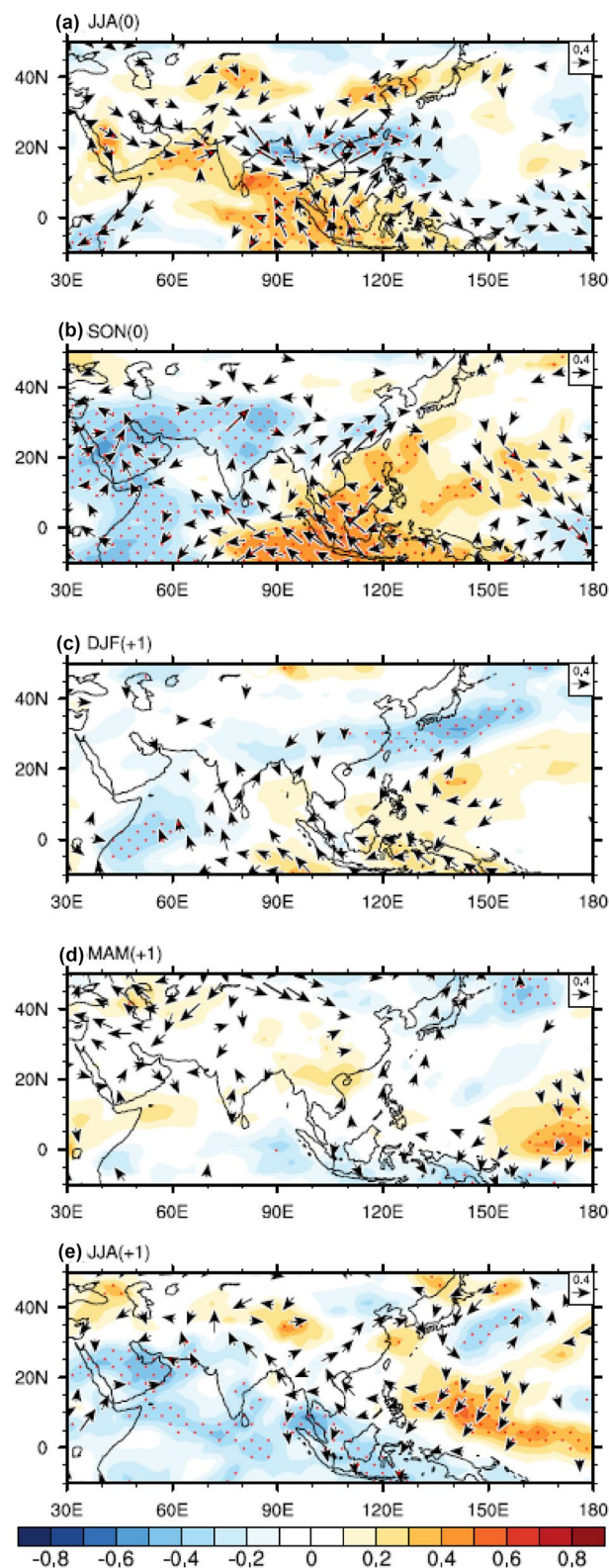

Fig. 4 Same as Fig. 3 but with respect to the unified monsoon index for summer. +1 indicates the ensuing year of the summer monsoon

the negative OLR value, is shown over SC, associated with cyclonic circulation. For the following autumn, a positive OLR maximum controls the SCS, but quickly weakens during the following season. During DJF(+1), in addition to the suppressed convection over the tropical region, we can also see the enhanced convection belt from SC to the east of Japan, which is the opposite of Fig. 2a, signifying the characteristics of a weak winter monsoon. Therefore, we can identify an out-of-phase relationship from JJA(0) to DJF(+1), which is similar to the results of an out-of-phase relationship shown in Fig. 3. According to Fig. 4d, the signal nearly vanishes during this spring, which may be attributed to the 'spring barrier' effect (Webster and Yang 1992). As a result, the signals in the following two seasons are hard to interpret. However, from summer to winter alone, the result is consistent with that when focusing on winter.

The seasonal relationships over SC are also confirmed by the lead-lag correlation map based on the time series of the unified monsoon index during summer: monsoon activities tend to have an out-of-phase relation from summer to winter, but become in-phase from winter to summer. Due to the similarity of seasonal relationships revealed in Figs. 3 and 4, the following analysis will focus only on winter, which means considering winter as the central season and studying its relationships with the previous and ensuing summer.

4 Forcing effects of ENSO and IO on seasonal relationships of monsoon activities between summer and winter

Since climate system memory cannot last long enough to preserve an anomalous signal through different seasons, the seasonal connection must be related to another long-term memory forcing system (Zhou and Chan 2007; Zhou et al. 2007a, b; Yuan et al. 2008a, b; Gu et al. 2009a, b; Wang et al. 2012), but the mechanism behind this connection is very complex. Some previous studies have revealed that the seasonal relationships of monsoon activities can be modulated by ENSO (Chang et al. 2000; Chen et al. 2000; Wu and Chan 2005b; Wang et al. 2011; Feng and Chen 2014; Wu et al. 2014); others have also emphasized the role of local SST anomalies or IO forcing in capturing the anomalous signals of the last season (Lau and Nath 2003; Lau et al. 2006; Li et al. 2010; Wang and Wu 2012; Wu et al. 2014); and some studies have also differentiated the relative role of local cold SST anomalies in the western Pacific and Indian Ocean basin mode (IOBM) in maintaining the anomalous anticyclonic circulation from the El Niño mature winter to the decaying summer (Wu et al. 2010).

We want to emphasize two questions here: what are the relative contributions of ENSO and IO forcings to monsoon seasonal transitions, and how does the IO modulate the relationship between the summer and winter monsoons?

4.1 ENSO and IO forcing

In order to investigate the ocean forcing effect, correlation analysis is also employed on SST fields, as shown in Fig. 5. The SST forcing fields represent mainly an evolution of a La Niña-like pattern over the East Pacific (EP), which starts in the preceding summer when the cold SST signal is developing off the coast of Peru, and ends the following summer. This La Niña-like pattern verifies that the ENSO cycle is vital to the connections between seasonal monsoon activities. At the same time, evident signals can also be identified over the IO. During SON (-1), a warm SST signal is located over the eastern tropical IO region, and a cold SST signal is dominant over the western part, signifying a typical negative IOD pattern (Fig. 5c). However, during the simultaneous winter and the following two seasons (Fig. 5d, e), the IOD pattern ends and an IOB cooling pattern dominates the tropical IO. According to lead-lag correlation maps, forcing effects from not only the Pacific region but also the IO can be confirmed. Therefore, these correlation analyses suggest that strong winter monsoons tend to be concurrent with a La Niña-like pattern over the EP; during the previous autumn, a negative IOD pattern is also evident, and during the ensuing spring, IOB cooling is dominant.

To further confirm the EP and IO forcing effects and discuss the potential seasonal connections, composite difference analysis is used, based on strong (1983, 1988, 1995, 1998, 2003, and 2007) and weak winter monsoon years (1982, 1984, 1991, 1993, 1997, 2002, 2004, 2009). Precipitation evolution over SC (107.5°E–120°E) is first examined to revisit the seasonal relationships between the two monsoon seasons, using GPCP and station data (Fig. 6a, b). A comparison of Fig. 6a, b shows that the evolution patterns are very similar, but the magnitude of the station data is greater. In the following discussion, the numbers − 1 and 0 have the same meaning as in the earlier correlation analysis. During the preceding summer, SC experiences less rainfall, which is the opposite of the Yangtze River region, and together they correspond to weak summer monsoon precipitation patterns according to the correlation distribution in Fig. 2c. Similarly, according to earlier findings, during strong winter monsoon years, there should be a negative precipitation belt between 20°N and 30°N (Fig. 2a), which is just evident in Fig. 6a, b. In the ensuing summer, the southern part of SC experiences more precipitation, contrary to the negative anomalies in the north, and similar to the strong summer monsoon pattern. So, from the previous summer to the ensuing summer, an out-of-phase relationship of weak summer monsoons with strong winter monsoons, and an in-phase relationship of

Fig. 5 Distribution of correlation coefficients of SST anomalies in lead-lag seasons with respect to the time series of the unified monsoon index for winter. Dotted areas are statistically significant at the 95% confidence level
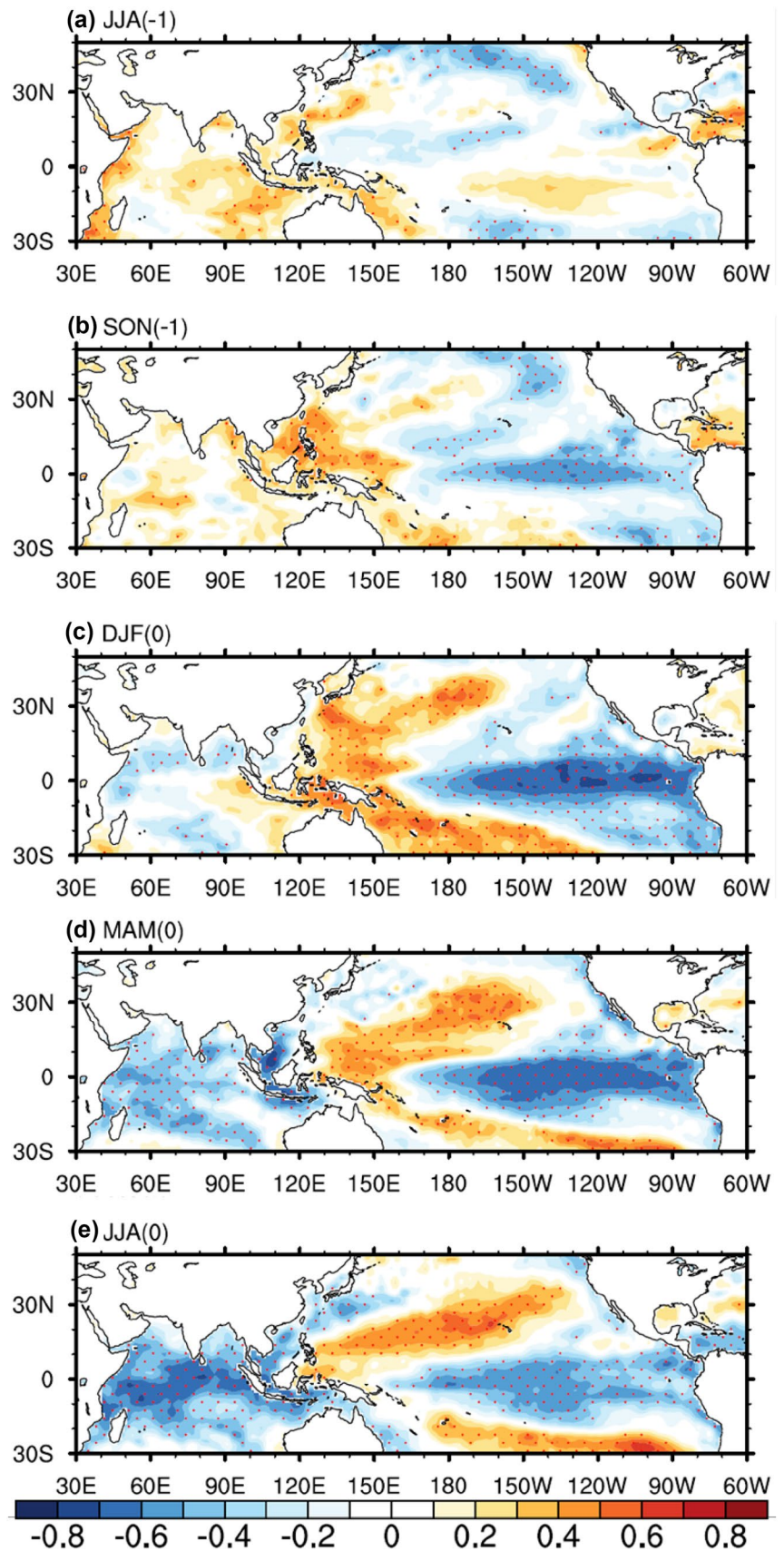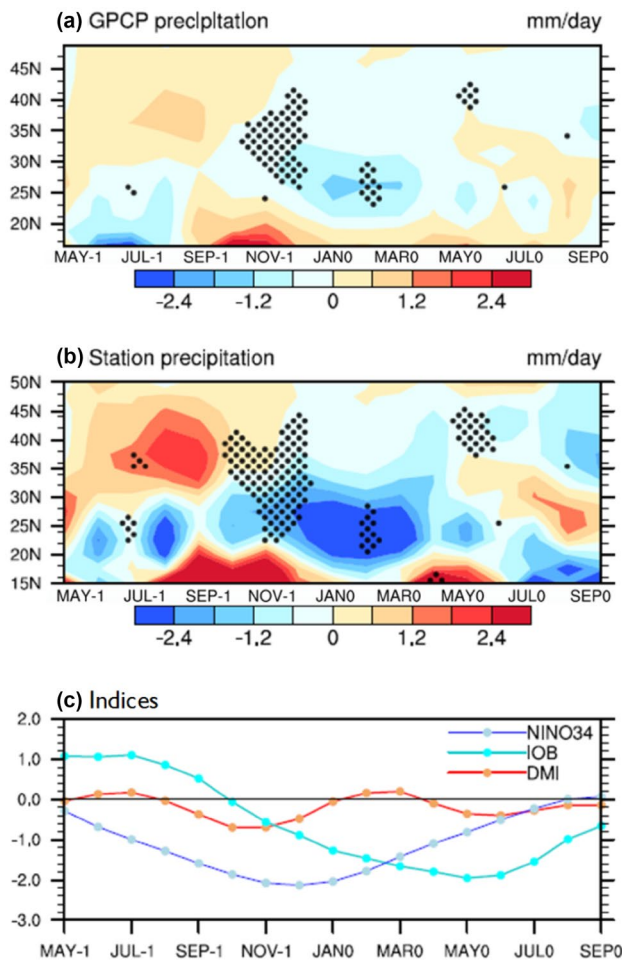
Fig. 6 Composite difference of precipitation anomalies over 107.5°E–120°E between strong and weak winter monsoon years based on **a** GPCP and **b** station data. Dotted areas are statistically significant at the 95% confidence level. **c** Composite evolution of Niño 3.4, IOB index, and dipole mode index (DMI), based on the difference between strong and weak summer monsoon. − 1 indicates the preceding year of the winter monsoon, 0 represents the same year

strong winter monsoons with strong summer monsoons can be clearly seen according to the evolution of precipitation.

During this whole process, EP and IO forcing effects can be identified in the evolution of the Niño 3.4, IOB, and DMI indices (Fig. 6c). From Niño 3.4, we can see that the negative ENSO event, a La Niña-like event, develops in the preceding spring and matures in the winter, and then after its peak stage, it decays quickly. However, in addition to ENSO forcing, a negative IOD is also evident during autumn, reflected by the negative DMI value, which might contribute to the out-of-phase relationship as well. During the decay stage of ENSO, the IOB cooling process is dominant and can persist even to the ensuing summer according to the evolution of the IOB index, showing that the IOB might have a crucial impact on the relationship of monsoon activities from winter to the ensuing summer.

4.2 Out-of-phase relationship from summer(− 1) to winter(0): ENSO and IOD forcing

In order to reveal how the seasonal connection is modulated by the EP and IO forcing effects, the composite circulation difference between strong and weak winter monsoon years is further investigated.

During the preceding summer, due to the development of a cold SSTA over the eastern tropical Pacific Ocean (Fig. 7a), an anomalous Walker circulation develops over the equatorial Pacific (Fig. 8a), but its ascending branch is relatively weak and confined to the south of 10°N (Fig. 8f). SC and the northern SCS are controlled by an anomalous descending motion, and a local meridional circulation is formed over the SCS region (Fig. 8f), where the location of descending motion (Fig. 9a) is consistent with that of a negative precipitation response (Fig. 7f). In the lower troposphere, 850 hPa wind fields show that an anticyclonic circulation pattern dominates over SC associated with high sea surface pressure (Fig. 7f). In the midtroposphere (Fig. 9a), a positive center of geopotential height is located over SC, indicating that the subtropical high is enhanced during this summer, so the monsoon convection is suppressed over this region (Zhou and Chan 2007).

During the transition autumn, a cooling SST anomaly gets stronger over the EP (Fig. 7b), and so does the anomalous Walker circulation (Fig. 8b), whose ascending branch also gets stronger and extends into higher latitudes (Fig. 8g). When the IOD pattern matures (Fig. 7b), an anomalous zonal circulation is also formed over the IO (Fig. 8b), triggering anomalous westerlies along the equator (Fig. 7g) in the lower troposphere. And to the north of the west-wind anomaly, a cyclonic circulation forms, controlling the Bay of Bengal (BOB) and SCS (Fig. 7g).

During the peak phase of ENSO, the cyclonic circulation over the WNP becomes strongest, and to its northwest there are northerly wind anomalies that can strengthen the northeasterly monsoon winds (Fig. 7h). Geopotential height fields at 500 hPa also show negative responses over the midlatitudes of EA, indicating a strong East Asian trough and strong winter monsoon activity (Fig. 9c). So the winter monsoon is strong over SC under the influence of the La Niña-like pattern, as expected from earlier findings (e.g., Li 1990).

In the higher troposphere (Fig. 9), starting in SON(− 1), a pair of cyclones is evident straddling the equator over the EP, indicating a Gill-type response (Gill 1980) to the cooling SSTA to its east. And this pattern becomes stronger during winter. Meanwhile, over the IO, a wedge-shaped circulation represents a Kelvin wave response produced by the cooling in the western tropical IO. Also, due to this heating sink, a wave-like pattern develops from the IO to EA (Fig. 9c), contributing to the anomalous precipitation pattern over EA (Fig. 7h). These signals also confirm that both ENSO
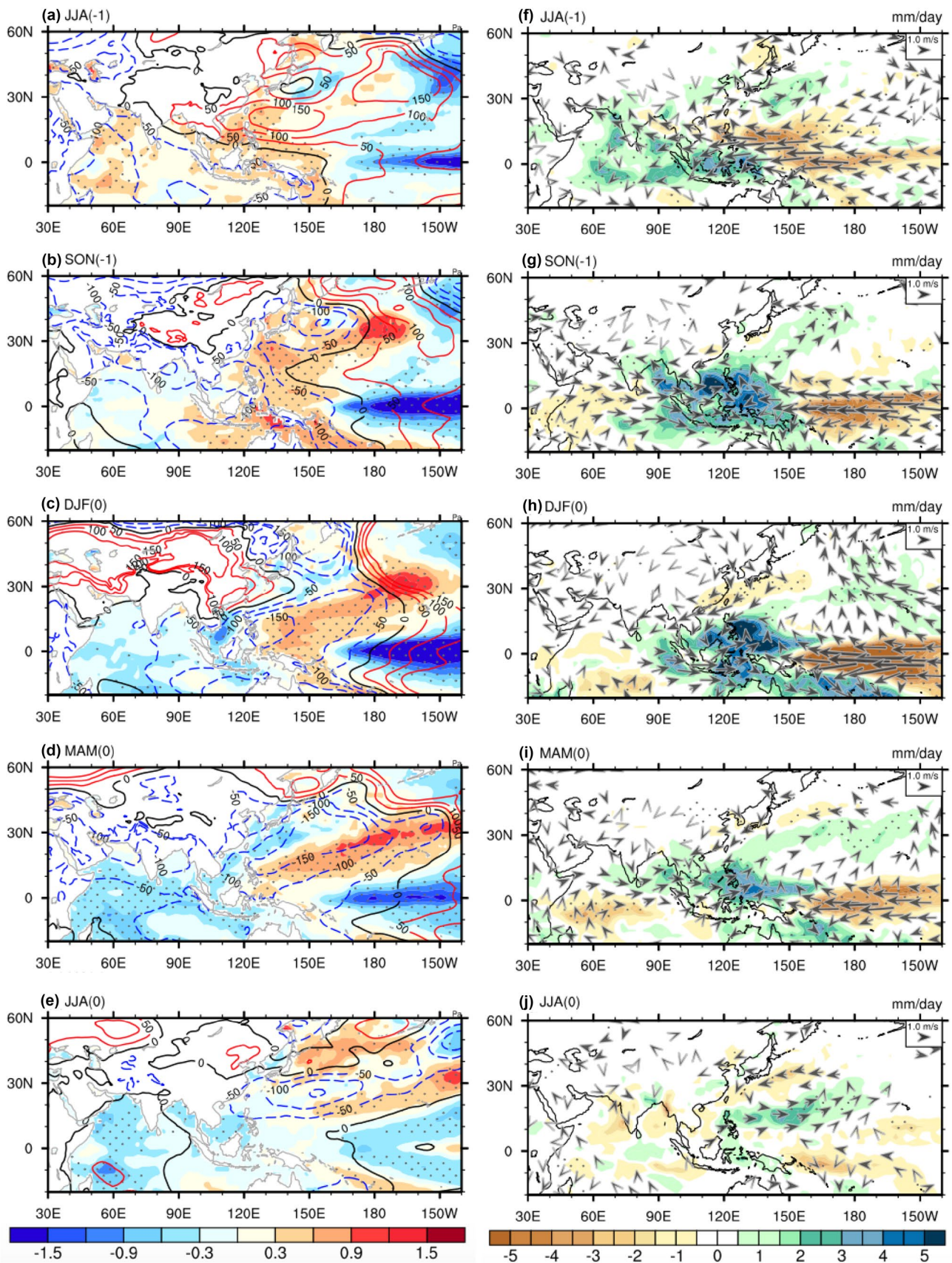
and IOD can have important influences on winter monsoon activity.

4.3 In-phase relationship from winter(0) to summer(0): ENSO and IOB forcing

As earlier composite evolution results indicate, a strong winter monsoon associated with a mature La Niña-like pattern can be expected to be followed by a strong summer monsoon. We can also deduce the mechanisms of the ENSO and IO forcing effect on this seasonal relationship from winter to the following summer according to the composite difference during the following two seasons. The cooling SSTA over the equatorial Pacific decays during the following two seasons, and starting in the spring, the SST mode over the IO changes to a whole-basin cooling mode (IOB cooling) (Fig. 7d, e). According to Xie et al. (2009), the anomalous SST condition of the tropical IO can act as a capacitor effect of ENSO and maintain the anomalous signals until the next summer. The theory is that the cooling tropical IO triggers a Kelvin wave response and induces southwest winds toward the WNP, thus causing convergence anomalies there, which is basically the mechanism of Kelvin wave-induced Ekman divergence but with an opposite sign (Xie et al. 2009; Wu et al. 2009). Seasonally, during the transition spring, due to a cold SSTA over the IO, anomalous descending motion is evident over the tropical IO (Fig. 8d), and it can induce a local meridional circulation with ascending motion over the SCS (Figs. 8i, 9d), causing positive precipitation responses over that region (Fig. 7i). During the following summer, a positive precipitation response can be seen over the Yangtze River, and a significant positive response is evident over the WNP. The anomalous cyclone is still evident over the WNP in the lower troposphere (Fig. 7j), and in the middle troposphere, a negative response can be seen (Fig. 9e), so these patterns are related to a weak subtropical high, which will benefit moisture transfer to SC (Zhou and Yu 2005). Under the control of this anomalous cyclone, monsoon activities over SC tend to be stronger than normal, so an in-phase relationship between strong winter monsoons and strong summer monsoons over SC can be identified.

Similarly, the impacts of ENSO and IOB can be further identified in the upper troposphere. During the following spring (Fig. 9d), a Gill-type response is still evident over the eastern equatorial Pacific. Over the IO, due to the change to IOB cooling, the heat sink location changes as well, so the

wave train patterns change, and the positive anomaly corresponds to the location of the South Asian High (SAH). This pattern indicates that the IOB can also influence the intensity of summer monsoon activity via modulating the SAH (e.g., Zhang and Wu 2001; Huang and Qian 2004). And the contribution of the forcing of IOB-like warming to the zonal expansion of the SAH has also been demonstrated by previous numerical model experiments (Zhou et al. 2009a).

5 Numerical simulations

In order to better demonstrate the mechanisms of how the anomalous forcing of ENSO, IOD, and IOB influences monsoon activities over SC and modulates the seasonal relationships, a five-layer anomalous dry atmospheric general circulation model (AGCM) with a horizontal resolution of T42 is used in this study, which consists of sigma levels 0.1, 0.3, 0.5, 0.7, and 0.9. Primitive equations are linearized by a realistic three-dimensional basic state, but nonlinearity is retained in the second-order perturbation terms of the prediction equations in the model. This model has been successfully used in many aspects of atmospheric studies: investigating the effect of the mean state on modulating anomalous forcing in the tropical Indo-Pacific (Wang et al. 2003); investigating the initiation of the boreal summer intraseasonal oscillation over the equatorial western IO (Jiang and Li 2005); examining the effect of vertical shear on the summertime synoptic-scale wave train in the western North Pacific (Li 2006); and identifying the modulation of the Pacific–Japan teleconnection on synoptic variability over the East Asia–western Pacific sector (Li et al. 2014). Details of the model can be found in the above studies.

In this study, we conduct two sets of experiments to simulate the coupling influence of IOD and ENSO, and IOB and ENSO, respectively. In each set of experiments, there are three runs: one in which both EP and IO forcing are added (EP & IO), one in which only IO forcing is added (IO), and one in which only EP forcing is added (EP). For each run, the model is linearized by adding the prescribed anomalous apparent heating patterns associated with EP and IO forcing on top of the early winter or early summer mean state, and integrating for 60 days. This produces a stable anomalous circulation pattern to investigate how the EP and IO influence monsoon circulation together and separately.

These heating patterns are based on the anomalous composite patterns of ENSO and IOD or IOB in reanalysis data, which are positive phases, in contrast to the earlier analysis that discussed mainly the influence of the negative phases of these modes. Because the peak season of IOD is autumn, and that of IOB is spring, we first plot the composite anomalous heating during autumn and spring (Fig. 10) to identify the anomalous heating patterns due to the forcing effects of
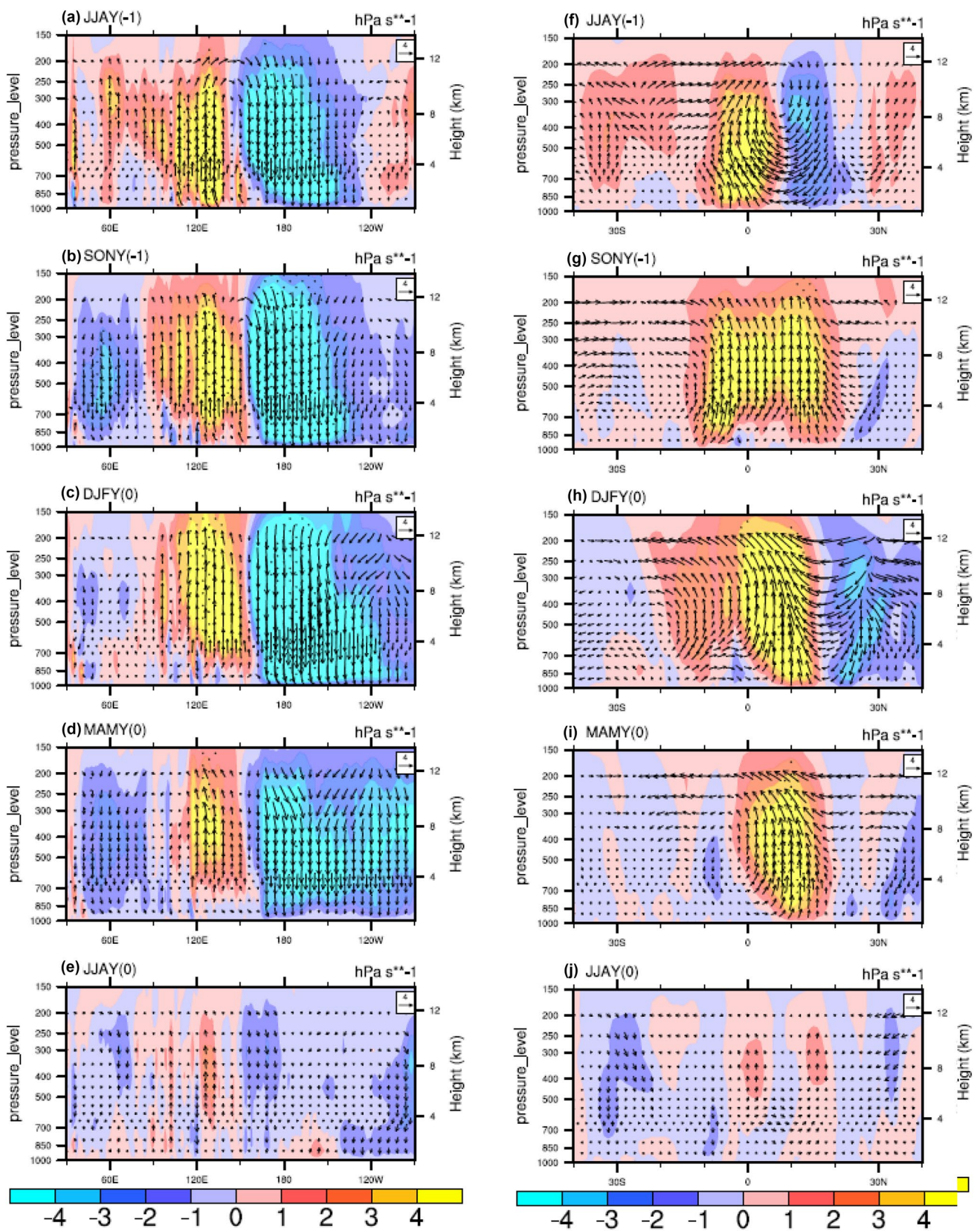
Fig. 8 Composite differences of **a–e** anomalous Walker circulation (averaged over 5°S–5°N), **f–j** anomalous meridional circulation (averaged over 100°E–140°E) from the preceding summer to the ensuing summer (JJA(−1)–JJA(0)) based on strong and weak winter monsoon years. Dotted areas are statistically significant at the 95% confidence level
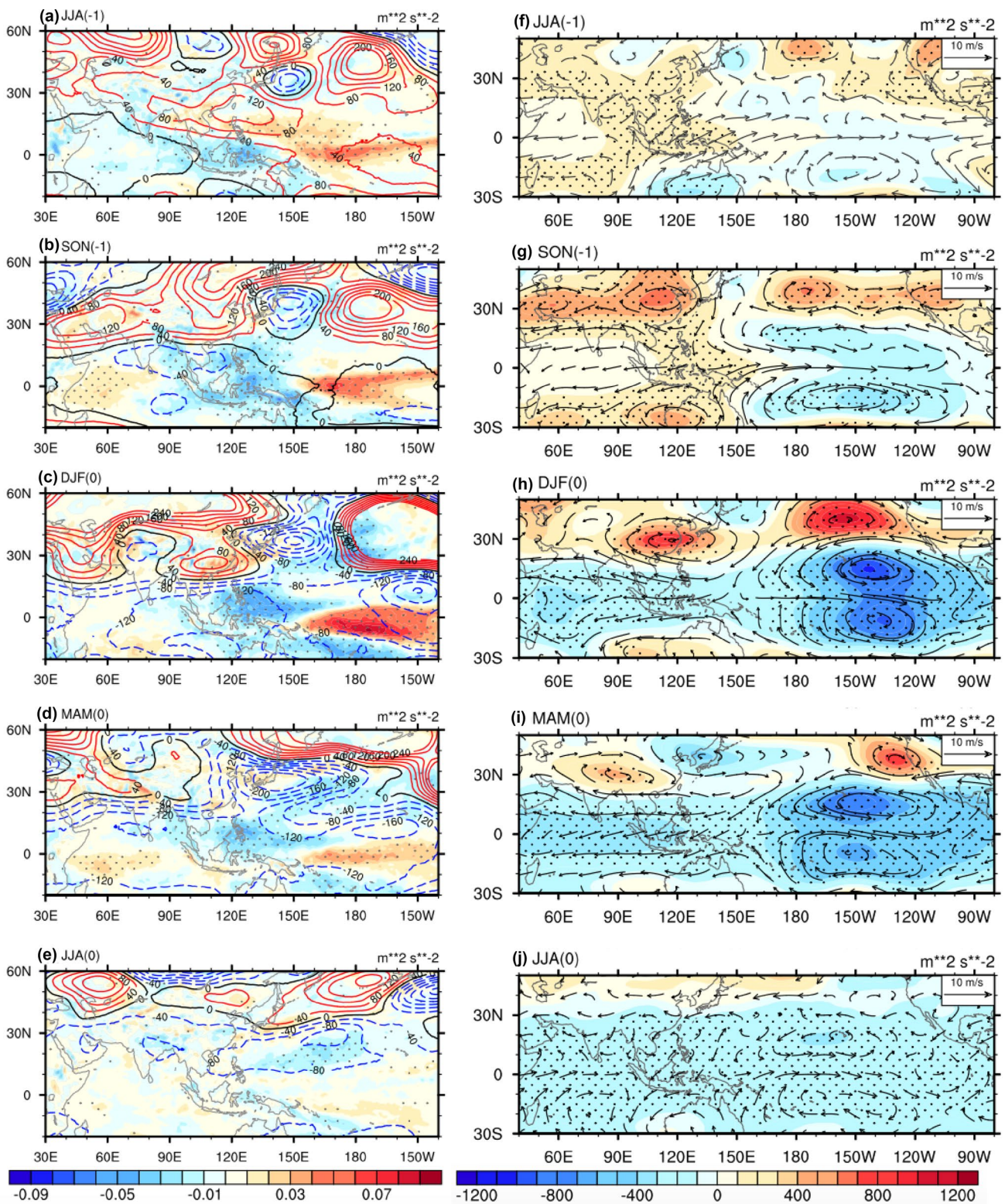
Fig. 9 Composite differences of **a**–**e** 500 hPa omega (shading, Pa/s) and geopotential height (contours), **f**–**j** 200 hPa winds (vectors) and geopotential height (shading) from the preceding summer to the ensuing summer (JJA(−1)–JJA(0)) based on strong and weak winter monsoon years. Dotted areas are statistically significant at the 95% confidence level
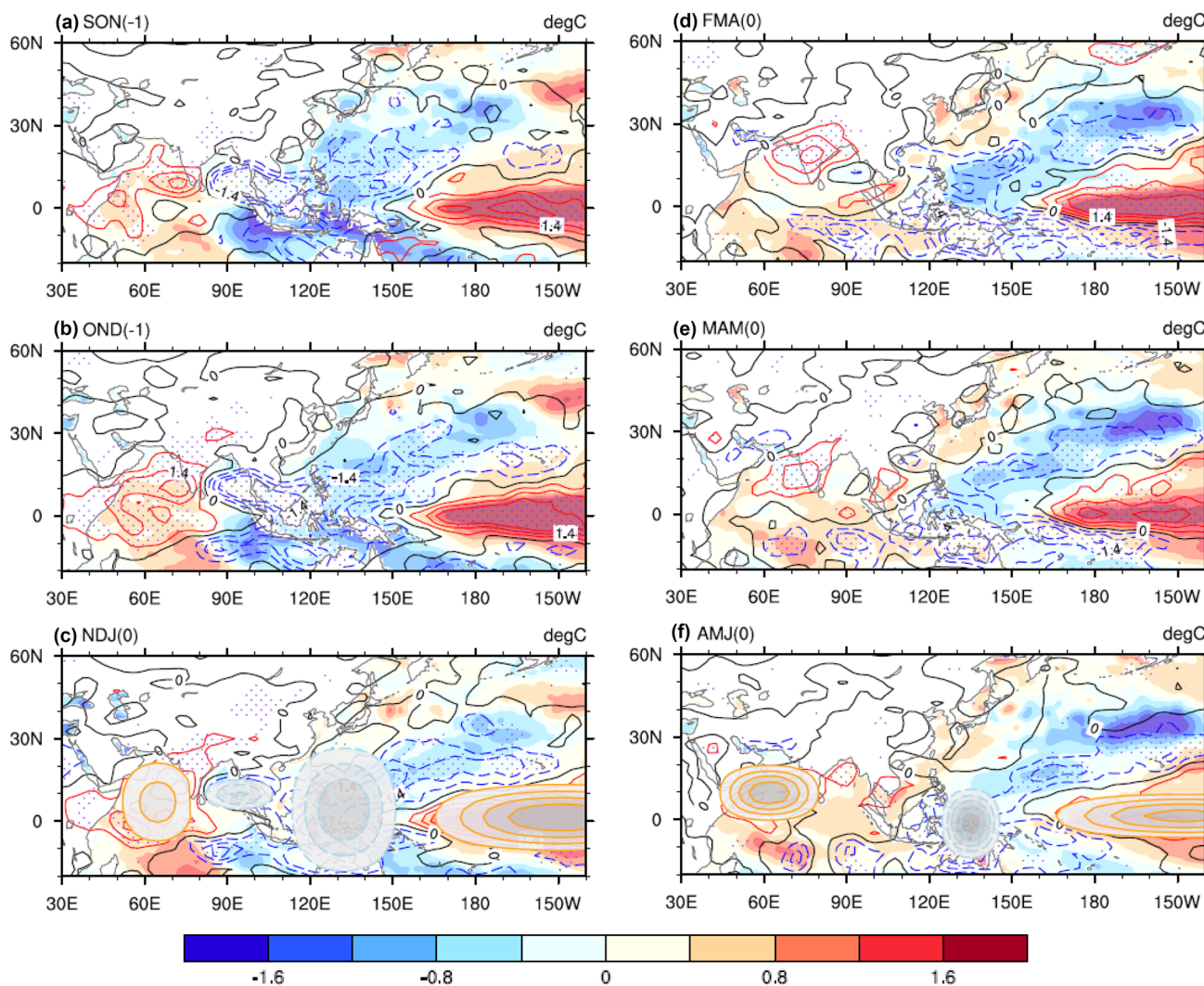
Fig. 10 Composites of SST anomalies (shading) and anomalous apparent heating (contours) during **a–c** autumn and **d–f** spring based on the coupling years of ENSO and IOD/IOB. Dotted areas are sta-
tistically significant at the 95% confidence level. In **c** and **f**, the gray shading represents heat sources (sinks) employed in the model simulation at the 0.5 sigma level with an interval of 0.2 K day^{-1}

IO and ENSO. During autumn (Fig. 10a–c), we can clearly see the evolution of the IOD pattern: it starts to establish in SON, reflected by the dipole of heating and SST patterns over the IO, and then reaches its maximum during OND, and decays during NDJ when the cooling center shrinks gradually. However, the locations of warming and cooling centers are consistent during these seasons. For the spring (Fig. 10d–f), when ENSO and IOB forcing occur together, the heat source is located over the Indian subcontinent during FMA, and then it expands to cover the whole equatorial IO, along with the evolution of IOB SST warming.

So, based on the evolution of anomalous heating patterns, and the aim of seeking the optimum seasons to investigate the effects of IO forcing on monsoon activities of the following season (winter or summer), we choose the NDJ and AMJ seasonal anomalous heating pattern to represent EP

and IO forcing associated with OND and MAM mean seasonal conditions to conduct these two sets of experiments, and the heating anomalies added in the model are shown in Fig. 10c, f.

Results of the first set of experiments, investigating the coupled influence of ENSO and IOD, are shown in Fig. 11. Comparing the EP&IO experiment with the observation field, we can see that this model simulates the basic characteristics over the equatorial region quite well, where the westerly wind anomalies, mainly due to the IOD forcing effect, and the easterly wind anomalies, mainly due to the ENSO forcing effect, are very similar to the observations. Although the performance of this model in the higher latitudes is not as good as in the lower latitudes, it can also simulate the southerly winds over EA and an anomalous anticyclone over the WNP, but with a little bias in the
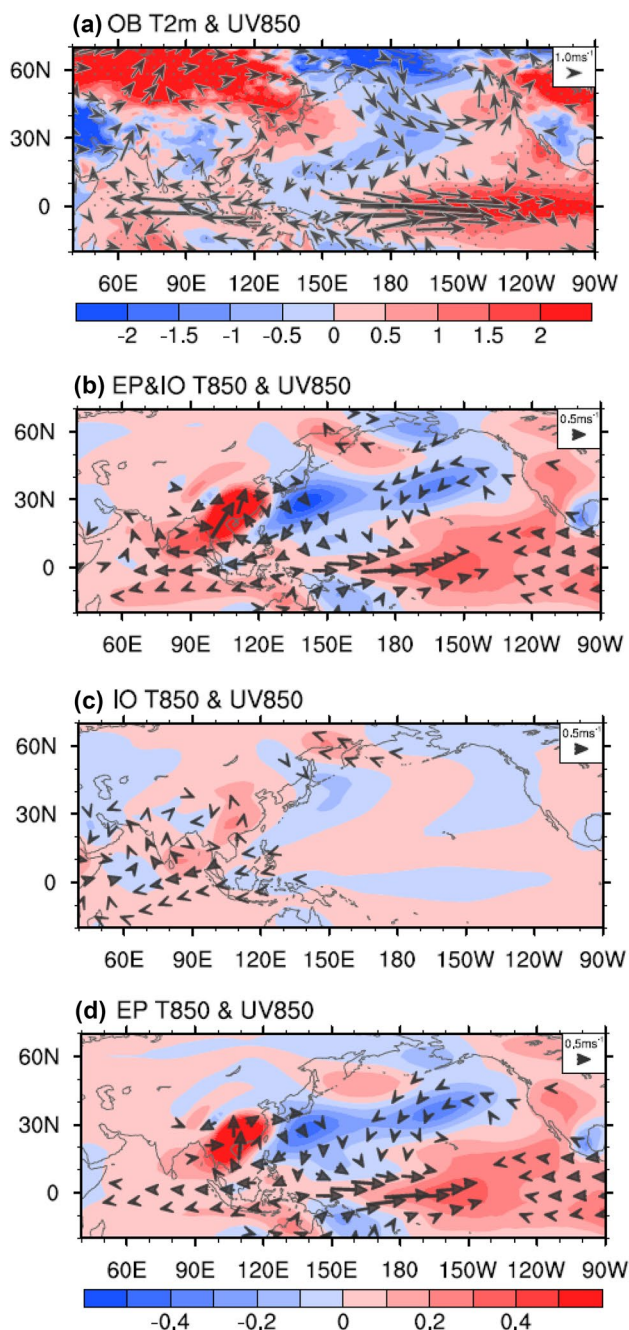
Fig. 11 850 hPa air temperature anomalies (shading; unit: K) and wind anomalies (vectors; showing only magnitudes > 0.04 m s⁻¹) in response to anomalous heat sources using a linearized AGCM prescribing the OND climatology and simulating IOD and ENSO forcing. Only those anomalous winds with speed over 0.2 m s⁻¹ are shown

locations. Meanwhile, the anticyclonic circulation patterns over the BOB and the Indochina peninsula are well captured in the experiments but are stronger than the observations. By separating these two modes, we can see that both the IOD and ENSO forcing can trigger southerly winds over

EA, which can weaken the northeasterly monsoon winds over this region. For the EP, the southerly winds are from the western edge of the anomalous anticyclone over the WNP, triggered by the descending branch of the anomalous Walker circulation due to the ENSO forcing. But for the IO, the southerly winds are directly induced by the heat sink region of the IOD pattern. At the same time, this also reveals that the anticyclonic circulations over the BOB and the Indochina peninsula are mainly a response to IOD forcing.

In the second set of experiments, we choose MAM as the basic circulation condition, and then add the IOB heat source pattern and anomalous ENSO heat pattern during AMJ to simulate the influence of these two modes on the summer monsoon circulation. The wind patterns over the tropical region are represented pretty well, as are those in the NDJ experiments. When only IOB warming is added in the experiment, we can see in Fig. 12c that the heat source induces a cyclonic pattern over the western IO, right over the location of the heating anomaly, and at the same time, it can draw the airflow to form westerly wind anomalies along the equator. Further, these patterns together can establish an anomalous anticyclone over the BOB and SCS region, which can influence the location of the subtropical high during summer, making it extend westward. Zhou et al. (2009a) also used numerical simulations to demonstrate that IO SST warming can increase convective heating in the equatorial IO/ Maritime Continent and lead to westward extension of the western Pacific subtropical high. Under these circumstances, the summer monsoon convection would be suppressed over SC and the SCS. But from Fig. 12d, we can see that with the modulation of only the ENSO pattern, there is limited influence over EA, which is consistent with the findings of previous studies that ENSO alone has hardly any influence on the summer circulation, because of the 'spring barrier' effect. Through these experiments, we find that mainly IOB warming has an effect on modulating the following summer climate, and as we know, IOB has a close coupling relationship with ENSO, so we can indirectly prove that IOB warming can act as a capacitor of the ENSO phenomenon, influencing monsoon activities over the SCS in the following summer and then enhancing the in-phase relationship between the weak winter monsoon and weak summer monsoon.

6 Summary and discussion

In this study, we investigate the seasonal relationships of monsoon activities over SC and discuss the modulation effects of IO and EP forcing. The primary results are illustrated schematically in Fig. 13. The unified monsoon index can well represent monsoon characteristics not only in winter but also in summer over SC. The time series of the unified monsoon index in summer and winter, and the
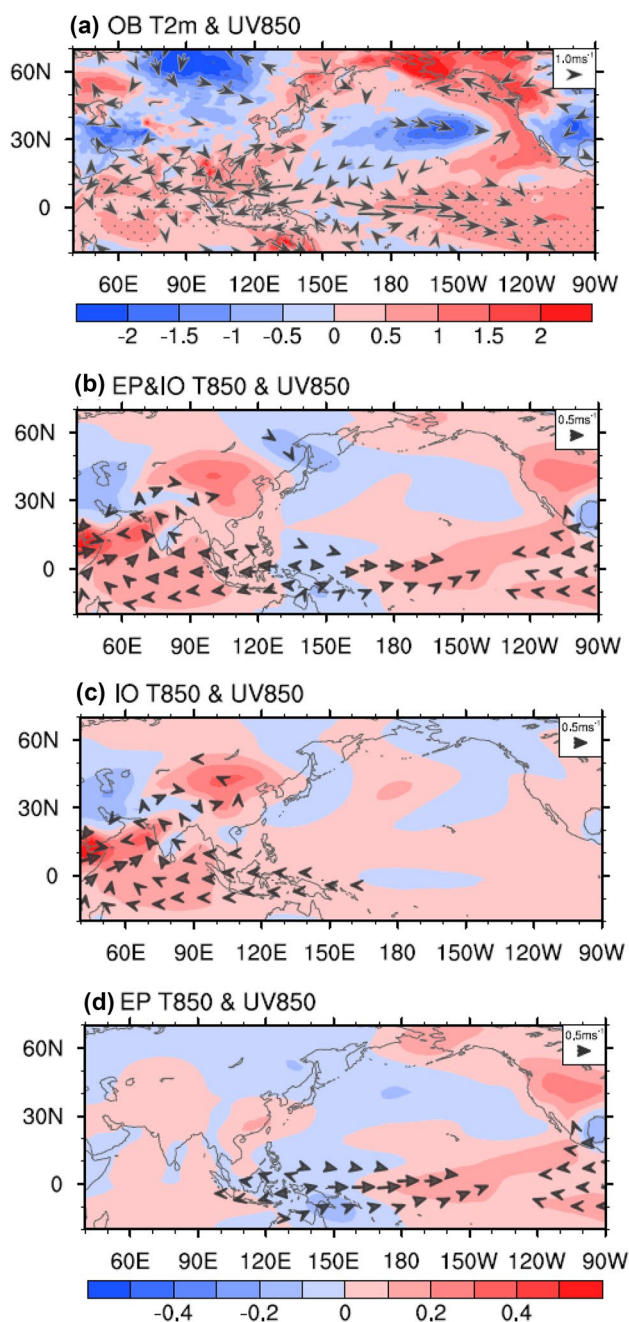
Fig. 12 Same as Fig. 11 but simulating IOB and ENSO forcing

seasonal connection of monsoon activities. The composite difference between strong and weak winter monsoons further confirms these seasonal linkages and reveals the modulating effects of ENSO, IOD, and IOB forcing. It is found that there is a tendency for a strong winter monsoon to be preceded by a weak summer monsoon, but followed by a strong summer monsoon over SC. A developing La Niña-like pattern over the EP during summer can enhance the Walker circulation, and then the above-normal ascending motion over the Maritime Continent can trigger an anomalous local meridional circulation, where the descending branch controlling SC suppresses the summer monsoon convection and weakens its activity. During winter, a strong winter monsoon is concurrent with the peak stage of the La Niña-like pattern, and under its modulation, through the strengthened Walker circulation, an anomalous cyclone can dominate the Philippine Sea and induce northerly winds on its western edge, strengthening the winter monsoon winds. During the following summer, this La Niña-like pattern decays quickly. A negative IOD is evident during the autumn and strengthens the Walker circulation over the IO, enhancing the ascending motion over the Maritime Continent and the intensity of the anomalous cyclone over the Philippine Sea. IOB cooling can capture the ENSO effect and strengthen monsoon activity during the ensuing summer by maintaining the anomalous cyclone over the WNP by the opposite mechanism of Kelvin wave-induced divergence (Xie et al. 2009).

The modulation effects of EP and IO forcing on monsoon activities in winter and summer can be verified by numerical simulations prescribing ENSO-like, IOD-like, and IOB-like heating patterns. The simulation results indicate that a positive ENSO event can weaken the winter monsoon winds but can hardly influence the following summer monsoon activity. However, it is found that the IOD can also weaken the winter monsoon winds during NDJ, and mainly the IOB contributes to the following weakened summer monsoon activity. Combined with earlier findings that summer monsoons tend to be stronger in the developing stage of positive ENSO events, the simulations also suggest that the IOD can enhance the out-of-phase relationship by further weakening the winter monsoon winds over EA, and the IOB can also enhance the in-phase relationship from winter to summer by weakening the following summer monsoon.

According to the seasonal relationships revealed by the unified monsoon index (Fig. 1c), the in-phase relationship from winter to summer may not be significant when there are 19 out 36 years following this relationship, only exceeding 1 year above the half. The reason for this may be that ENSO plays an important role in forcing with asymmetric patterns between positive and negative events. The seasonal relationship between winter monsoons and the ensuing summer monsoons was revisited under different phases of ENSO forcing (Table 1). According to Table 1, an in-phase

correlation analysis of the unified monsoon index, found that from summer to winter, monsoon activities tend to have an out-of-phase relationship, while from winter to summer, they tend to be in-phase. These seasonal relationships can provide further information about variation in monsoon activities and thus improve the seasonal prediction of monsoon activities over SC.

Lead-lag correlation maps between the winter monsoon index and the SST forcing field reveal the important roles of ENSO events and IOD and IOB forcing effects in the

Fig. 13 Schematic illustration of seasonal relationships of monsoon activities over South China, and the timing of ENSO and IO forcing effects
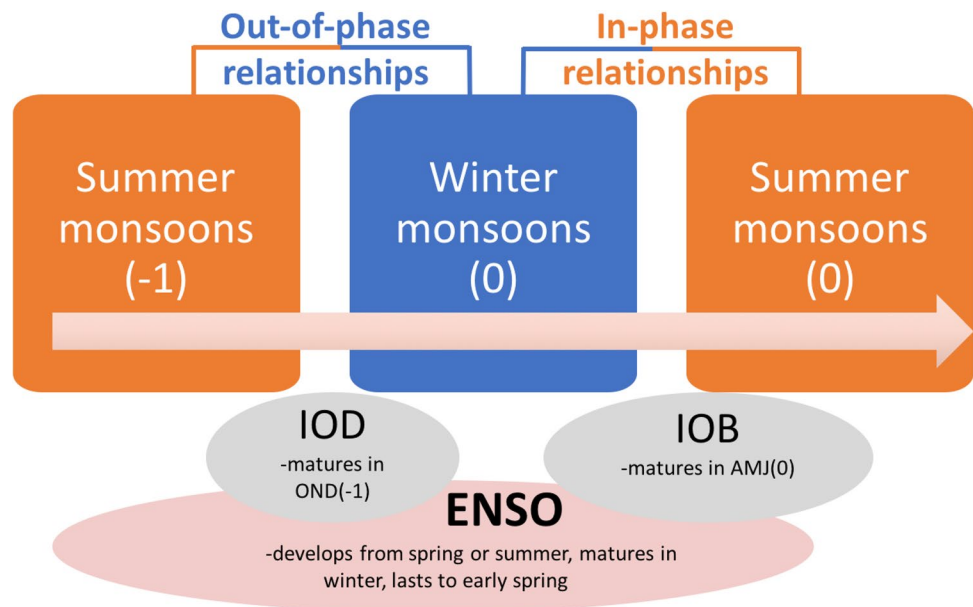

Table 1 Seasonal relationship from winter to summer and its probability under the influence of positive and negative ENSO events

From winter to summer	In-phase		Out-of-phase	
ENSO phase	Num. of years	Probability	Num. of years	Probability
ENSO+	8	0.8	2	0.2
ENSO−	5	0.417	7	0.583

relationship is much more dominant under the influence of positive ENSO events, with an occurrence probability of 0.8, while there is nearly no significant tendency for a seasonal phase relation under the influence of negative events. Besides the forcing modes discussed in this study, other possible contributions may also be important to the seasonal relationships of monsoon activities. Further work is needed to compare the different underlying mechanisms behind the in-phase and out-of-phase relationships of winter and summer monsoons.

On the other hand, in the composite maps (Figs. 7, 8, 9), the signals during the ensuing summer (JJA(0)) are also less significant than in other seasons. In order to further verify the roles of these three modes in the seasonal linkage from winter to the ensuing summer, partial correlation is also conducted in this study using the indices in peak seasons of each forcing mode correlated with precipitation in the ensuing summer, with results shown in Fig. 14. Compared with the correlation between indices and precipitation individually, the partial correlation patterns are quite similar to those in the correlation map, only with changes in magnitude. It is found that the contribution of ENSO to summer monsoon precipitation is less significant than the contribution of IO forcing in the partial correlation map, which proves that IO forcing is independent from ENSO to some extent. Yang et al. (2015) also illustrated that internal variability has the leading effect in modulating the IOD mode, compared to ENSO forcing. And IOB is also an internal mode contributed by inter-basin ocean–atmosphere feedback, as indicated by the NoENSO model simulation results from Kosaka et al. (2013). Meanwhile, the IOD influences mainly the precipitation over the Yangtze River and central China. And the IOB can significantly undermine the precipitation over the SCS and North China, but benefit the precipitation over eastern coastal China and southwestern China. Therefore, we can confirm that the IO influences the intensity of the monsoon in the following summer. But the questions of why IOD impacts show a basically opposite pattern from those of IOB over most of China, and of what their different roles are in modulating the relationship of monsoon activities from winter to summer need further investigation.
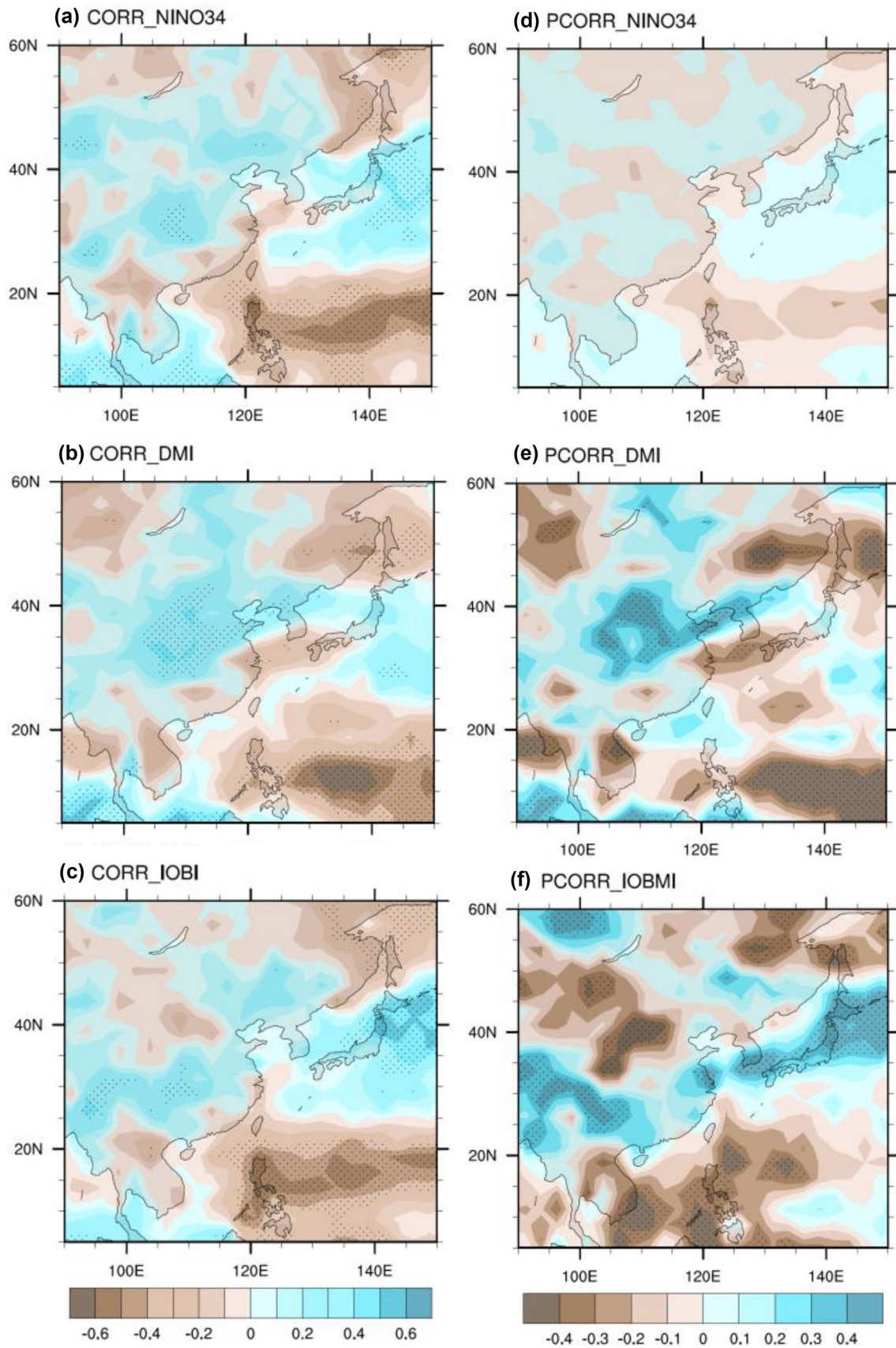
Fig. 14 **a–c** Correlations and **d–f** partial correlations of JJA(0) precipitation with (upper) DJF Niño 3.4, (middle) SON DMI, and (bottom) AMJ IOB index

References

Chan JCL, Zhou W (2005) PDO, ENSO and the early summer monsoon rainfall over South China. Geophys Res Lett 32:L08810. https://doi.org/10.1029/2004GL022015

Chang C-P (2004) East Asian monsoon. World Scientific, Singapore, pp 88–89

Chang C-P, Zhang Y, Li T (2000) Interannual and interdecadal variations of the East Asian summer monsoon and tropical Pacific SSTs. Part 1: roles of the subtropical ridge. J Clim 13:4310–4325

Chen W, Graf H-F, Huang RH (2000) The interannual variability of East Asian winter monsoon and its relation to the summer monsoon. Adv Atmos Sci 17:68–74

Chen W, Feng J, Wu R (2013) Roles of ENSO and PDO in the link of the East Asian winter monsoon to the following summer monsoon. J Clim 26:622–635

Cheung HN, Zhou W, Shao YP, Chen W, Mok HY, Wu MC (2013) Observational climatology and characteristics of wintertime atmospheric blocking over Ural-Siberia. Clim Dyn 41:63–79

Dee D, Uppala S, Simmons A, Berrisford P, Poli P (2011) The ERA-Interim reanalysis: configuration and performance of the data assimilation system. Q J R Meteorol Soc 137:553–597

Feng J, Chen W (2014) Interference of the East Asian winter monsoon in the impact of ENSO on the East Asian summer monsoon in decaying phases. Adv Atmos Sci 31:344–354

Gill AE (1980) Some simple solutions for heat-induced tropical circulation. Q J R Meteorol Soc 106:447–462

Gu W, Li C, Li W, Zhou W, Chan JCL (2009a) Interdecadal unstationary relationship between NAO and east China's summer precipitation patterns. Geophys Res Lett 36:L13702

Gu W, Li C, Wang X, Zhou W, Li W (2009b) Linkage between mei-yu precipitation and North Atlantic SST on the decadal timescale. Adv Atmos Sci 26:101–108

Huang YY, Qian YF (2004) Relationship between South Asian High and characteristic of precipitation in mid and lower reaches of the Yangtze River and North China. Plateau Meteorol 23:68–74

Jiang XA, Li T (2005) Reinitiation of the boreal summer intraseasonal oscillation in the tropical Indian Ocean. J Clim 18:3777–3795

Kalnay E et al (1996) The NCEP/NCAR 40-year reanalysis project. Bull Am Meteorol Soc 77:437–471

Kosaka Y, Xie S-P, Lau N-C, Vecchi GA (2013) Origin of seasonal predictability for summer climate over the northwestern Pacific. Proc Natl Acad Sci USA 110:7574–7579

Lau N-C, Nath MJ (2003) Atmosphere–ocean variations in the Indo-Pacific sector during ENSO episodes. J Clim 16:3–20

Lau N-C, Leetmaa A, Nath MJ (2006) Attribution of atmospheric variations in the 1997–2003 period to SST anomalies in the Pacific and Indian Ocean basins. J Clim 19:3607–3628

Lee H-T, Gruber A, Ellingson RG, Laszlo I (2007) Development of the HIRS outgoing longwave radiation climate dataset. J Atmos Ocean Technol 24:2029–2047

Leung MYT, Cheung HHN, Zhou W (2017) Meridional displacement of the East Asian trough and its response to the ENSO forcing. Clim Dyn 48:335–352

Li CY (1989) Warmer winter in eastern China and El Niño. Chin Sci Bull 34:1801–1805

Li CY (1990) Interaction between anomalous winter monsoon in East Asia and El Niño events. Adv Atmos Sci 7:36–46

Li T (2006) Origin of the summertime synoptic-scale wave train in the western North Pacific. J Atmos Sci 63:1093–1102

Li S, Lu J, Huang G, Hu K (2008) Tropical Indian Ocean basin warming and East Asian summer monsoon: a multiple AGCM study. J Clim 21:6080–6088

Li CY, Pan J, Que Z (2010) Variation of the East Asian monsoon and the tropospheric biennial oscillation. Chin Sci Bull 56:70–75

Li XZ, Wen ZP, Zhou W (2011) Long-term change in summer water vapor transport over South China in recent decades. J Meteorol Soc Jpn 89A:271–282

Li RCY, Zhou W, Li T (2014) Influences of the Pacific–Japan teleconnection pattern on synoptic-scale variability in the western North Pacific. J Clim 27:140–154

Li T, Wang B, Wu B, Zhou T, Chang CP, Zhang R (2017) Theories on formation of an anomalous anticyclone in western North Pacific during El Niño: a review. J Meteorol Res 31:987–1006

Liu YY, Wang L, Zhou W, Chen W (2014) Three Eurasian teleconnection patterns: spatial structures, temporal variability, and associated winter climate anomalies. Clim Dyn 42:2817–2839

Lu E, Chan JCL (1999) A unified monsoon index for South China. J Clim 12:2375–2385

Reynolds RW et al (2002) An improved in situ and satellite SST analysis for climate. J Clim 15:1609–1625

Wang L, Wu R (2012) In-phase transition from the winter monsoon to the summer monsoon over East Asia: role of the Indian Ocean. J Geophys Res 117:1–16

Wang B, Wu R, Fu X, Wang B, Wu R, Fu X (2000) Pacific-East Asian teleconnection: how does ENSO affect East Asian climate? J Clim 13:1517–1536

Wang B, Wu R, Li T (2003) Atmosphere–warm ocean interaction and its impacts on Asian–Australian monsoon variation. J Clim 16:1195–1211

Wang B, Lee J-Y, Kang I-S, Shukla J, Kug J-S, Kumar A, Schemm J, Luo J-J, Yamagata T, Park C-K (2008) How accurately do coupled climate models predict the leading modes of Asian–Australian monsoon interannual variability? Clim Dyn 30:605–619

Wang X, Wang C, Zhou W, Wang D, Song J (2011) Teleconnected influence of North Atlantic sea surface temperature on the El Niño onset. Clim Dyn 37:663–676

Wang X, Wang D, Zhou W, Li C (2012) Interdecadal modulation of the influence of La Niña events on mei-yu rainfall over the Yangtze River valley. Adv Atmos Sci 29:157–168

Wang B, Xiang B, Lee J-Y (2013) Subtropical high predictability establishes a promising way for monsoon and tropical storm predictions. Proc Natl Acad Sci USA 110:2718–2722

Wang L, Chen, Zhou W (2014) Assessment of future drought in Southwest China based on CMIP5 multimodel projections. Adv Atmos Sci 31:1035–1050

Webster PJ, Yang S (1992) Monsoon and ENSO: selectively interactive systems. Q J R Meteorol Soc 118:877–926

Wei K, Chen W, Zhou W (2011) Changes in the East Asian cold season since 2000. Adv Atmos Sci 28:69–79

Wu MC, Chan JCL (2005a) Observational relationships between summer and winter monsoons over East Asia. Part I: basic framework. Int J Climatol 25:437–451

Wu MC, Chan JCL (2005b) Observational relationships between summer and winter monsoons over East Asia. Part II: results. Int J Climatol 25:453–468

Wu B, Zhou T, Li T (2009) Seasonally evolving dominant interannual variability modes of East Asian climate. J Clim 22:2992–3005

Wu B, Li T, Zhou T (2010) Relative contributions of the Indian Ocean and local SST anomalies to the maintenance of the

western North Pacific anomalous anticyclone during the El Niño decaying summer. J Clim 23:2974–2986

Wu R, Huang G, Du Z (2014) Cross-season relation of the South China Sea precipitation variability between winter and summer. Clim Dyn 43:193–207

Xie S, Hu K, Jan H, Tokinaga H, Du Y, Huang G, Sampe T (2009) Indian Ocean capacitor effect on Indo-western Pacific climate during the summer following El Niño. J Clim 42:730–747

Xie S-P, Kosaka Y, Du Y, Hu K, Chowdary JS, Huang G (2016) Indo-western Pacific Ocean capacitor and coherent climate anomalies in post-ENSO summer: a review. Adv Atmos Sci 33:411–432

Yang Y et al (2015) Seasonality and predictability of the Indian Ocean dipole mode: ENSO forcing and internal variability. J Clim 28:8021–8036

Yasunari T (1991) The monsoon year—a new concept of the climatic year in the tropics. Bull Am Meteorol Soc 72:1331–1338

Yuan Y, Zhou W, Chan JCL, Li C (2008a) Impacts of the basin-wide Indian Ocean SSTA on the South China Sea summer monsoon onset. Int J Climatol 28:1579–1587

Yuan Y, Yang H, Zhou W, Li C (2008b) Influences of the Indian Ocean dipole on the Asian summer monsoon in the following year. Int J Climatol 28:1849–1859

Yuan Y, Zhou W, Yang H, Li C (2008c) Warming in the northwestern Indian Ocean associated with the El Niño event. Adv Atmos Sci 25:246–252

Zhang Q, Wu G (2001) The large area flood and drought over the Yangtze River valley and its relation to the South Asian high. Acta Meteorol Sin 59:569–577 (**in Chinese**)

Zhou W, Chan JCL (2007) ENSO and the South China Sea summer monsoon onset. Int J Climatol 27:157–167

Zhou T, Yu R (2005) Atmospheric water vapor transport associated with typical anomalous summer rainfall patterns in China. J Geophys Res 110:D08104

Zhou W, Li C, Wang X (2007a) Possible connection between Pacific Oceanic interdecadal pathway and East Asian winter monsoon. Geophys Res Lett 34:L01701

Zhou W, Wang X, Zhou TJ, Li C, Chan JCL (2007b) Interdecadal variability of the relationship between the East Asian winter monsoon and ENSO. Meteorol Atmos Phys 98:283–293

Zhou T, Yu R, Zhang J, Drange H, Cassou C, Deser C, Hodson DLR, Sanchez-Gomez E, Li J, Keenlyside N, Xin X, Okumura Y (2009a) Why the western Pacific subtropical high has extended westward since the late 1970s. J Clim 22:2199–2215

Zhou T, Wu B, Wang B (2009b) How well do atmospheric general circulation models capture the leading modes of the interannual variability of the Asian–Australian monsoon? J Clim 22:1159–1173